Voltage-Dependent-Capacitor Control of Wireless Power Transfer (WPT)

Sahar Borafker, Miriam Drujin, and Shmuel (Sam) Ben-Yaakov*, *IEEE, Life Fellow*
Department of Electrical and Computer Engineering Ben-Gurion University of the Negev, Beer Sheva, Israel
Sahar37@gmail.com, Mirit_dr@hotmail.com, sby@bgu.ac.il, http://www.ee.bgu.ac.il/~pel

Abstract. A proposed voltage-dependent-capacitor tuning method for WPT systems was studied analytically, by simulation and verified experimentally. The circuit implementation applies common ferroelectric ceramic capacitors as voltage dependent elements. The experimental results on a mockup of autonomous mini-submarine charging, suggest that commercial ceramic capacitors are a viable option for tuning WPT.

Keywords - Wireless power transfer, Undersea, Resonant converter, Power Electronics.

I. INTRODUCTION

Wireless power transfer (WPT) has been proposed and is now being applied in a multitude of applications ranging from charging of low power devices as pacemakers and cellular phones to high power level equipment such as cars, buses, and submarines [1-3]. The primary design objectives of WPT are high input to output gain and high efficiency. A number of approaches have been suggested to meet these goals including: control of input voltage, frequency tuning, possible communication between receiver and transmitter, and others [4]. Tuning can be accomplished by frequency adjustment and conversely or concurrently by changing the resonant capacitance of one of the antennas [5]. This study explored the possibility of using a voltage dependent capacitor for WPT tuning. The advantage of voltage dependent capacitors control is the infinite resolution (limited only by noise) that can be achieved, as compared to the discrete capacitances obtained by a bank of switched capacitors [5]. Although the target application is charging an autonomous mini-submarine, the proposed methods is general and applicable to other WPT cases as well as to resonant converters. This paper covers the general aspects of the proposed variable-voltage capacitor control.

II. THE VOLTAGE-DEPENDENT CAPACITOR CONTROLLED WPT MODEL

Two alternative models can be used to describe a WPT system. One is based on the mutual inductance concept [6] and the other, which is applied here, on a transformer equivalent circuit. In this model (Fig. 1a) which is drawn here, in the interest of brevity, for equal inductances of primary and secondary, the distance between the antennas is affecting the coupling coefficient k. This coefficient, in turn, sets the value of the leakage inductances $Llkg1=Llkg2=L1(1-k)$, and the common inductance reflected to the primary L1=kLp, where Lp is the total inductance seen at the primary with an open secondary. The parasitic resistances of the primary and secondary are neglected in this generic circuit. Capacitors, Cp and Cs, are used to tune the circuit.

The load, which is normally nonlinear, is represented in this small signal model by an equivalent resistor Rac, that is obtained by applying the first harmonics approximation [7]. This approximation is also used to represent the input voltage (which will normally be a square wave) as a sinusoidal source Vin.

In way of simplification, and to help explain the approach taken in this study, consider the case in which the voltage at point Va (Fig. 1a) is controlled to be a constant voltage of a fixed frequency fs. Applying Thevenin's theorem with respect to this virtual source, the equivalent circuit (Fig. 1b) can now

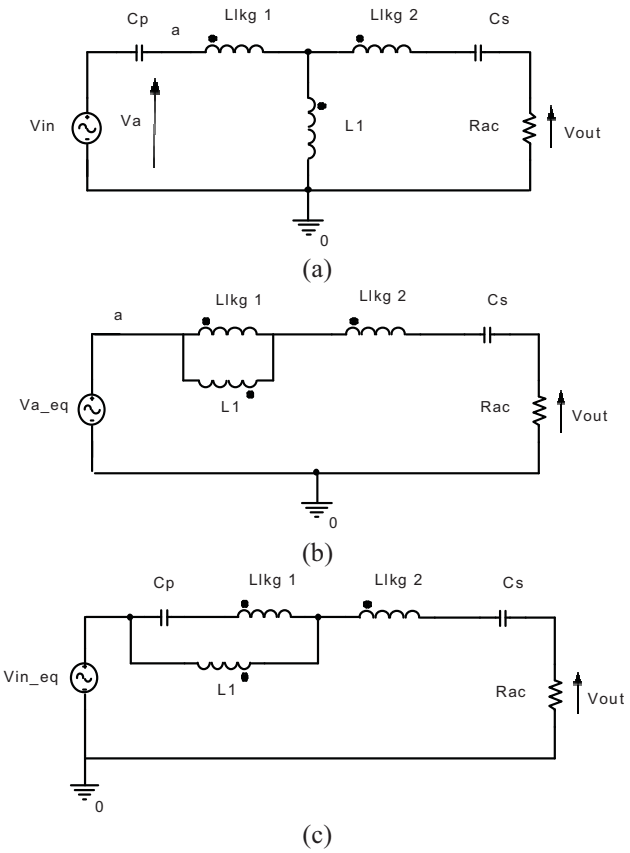

Fig. 1. Simplified Thevenin equivalent circuit model of a WPT system. (a) The transformer equivalent circuit. (b) Thevenin equivalent. (c) Taking primary capacitor C_p into account.

978-1-5386-6378-3/18/$31.00 ©2018 IEEE

be modelled as a basic series resonant network fed by an equivalent source Va_eq.

$$V_{a\_eq} = \frac{kL_p}{kL_p + (1-k)L_p} = V_a K \tag{1}$$

From this presentation it becomes clear that the maximum power transfer can be reached by adjusting Cs to

$$C_s = \frac{1}{4\pi^2 f_s (1-k^2) L_p} \tag{2}$$

and that the transfer ratio Vo/Va at resonance will be k.

Taking Cp into account in the Thevenin equivalent model, the situation becomes somewhat more complex (Fig. 1c). The equivalent circuit now includes a more elaborate network at the input and the equivalent source (Vin_in) is frequency dependent. However, for a given fixed frequency, the series input network may be represented by an inductor or capacitor. Hence, maximum power transfer can again be reached by adjusting Cs such that the total assembly will be at resonant at the drive frequency fs. The fact that the equivalent input voltage expression describes, in fact, a multi-resonant circuit, may lead to a voltage gain in some operating points. Consequently, the voltage transfer ratio may reach values above k. This cab be see by examining the voltage transfer ration between the input and the high side of L_1 when the load impedance is large, as given in (3):

$$\frac{V_{mid}}{V_{in}} = \frac{4\pi^2 L_1 C_p}{4\pi^2 C_p (L_1 + L_{lkg1}) - 1} \tag{3}$$

The above fundamental understanding is the basic idea behind the proposed tuning method: to tune to maximum power delivery by adjusting Cs at the receiver. The generic topology of the proposed implementation (Fig. 2) includes a power driver, a tuned transmitting and receiving antennas, a load, and a bias voltage of high output impedance by which the voltage-dependent capacitor C2 is controlled. Fig. 2 does not include details of the control loop or possible communication between the load and source. The purpose of C3 is to block the DC path from bias driver to the antenna. C3 could be a fixed or voltage dependent capacitor.

Considering the many degrees of freedom involved, SPICE simulation could be used advantageously to reach an optimum design for a given application.

III. SPICE SIMULATION

For the sake of brevity, dictated by the limited space available in this digest, simulation is shown here only for the private case of the experimental set up. The loop antennas parameters were as follows.

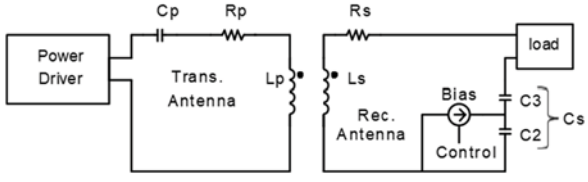

Fig. 2. Proposed variable capacitor controlled WPT system.

Primary inductance, Lp= 103μH, primary parasitic resistance: Rp=300mΩ. Secondary inductance Ls=54uH, secondary parasitic resistance Rp=300mΩ. A preliminary simulation search for optimum parameters yielded: Operating frequency 45kHz, load resistance 5Ω and Cp= 0.47μF. The target power level for the proof-of-concept experiment was 10W.

Fig. 3. Shows the simulation results of a parameter sweep on Cs (equal to C2 in series with C3) for three coupling coefficients k= 0.2, 0.5, 0.7 which cover a wide range of applications. The plots reveal that maximum power transfer can be reached in each case by adjusting Cs as proposed. Furthermore, the transfer voltage ratios, reached for each coupling coefficient, is close to the value of k as expected.

IV. THE VOLTAGE-DEPENDENT CAPACITOR

The proposed approach clearly hinges on the availability of voltage-dependent capacitors for realizing the suggested concept. As it turns out, the common and highly popular ceramic capacitors, fill the bill. Ferroelectric ceramic capacitors (designated as Class II and Class III by the industry) are highly voltage dependent. Fig. 4a is a copy of the curve given in the manufacturer's (Murata) data sheet for one of the experimental capacitors used in this study (Murata, GRM31MR72A474KA35). It is clear that the possible percentage change of this capacitor is compatible with Cs required percentage range, for a given coupling coefficient, as found by the simulation run (Fig. 3). Furthermore, this single capacitor is capable of carrying a current in the order of about 2Arms (Fig. 4b) with a temperature rise of about $30C^0$, since two capacitors were used in parallel, the current could safely reach 4Arms.

An extended WPT capacitor control option which is considered in this study, is the combination of discrete and continuous variable capacitance control. In this case, the variable capacitor is composed of a bank of switch selectable capacitors in parallel to a voltage dependent capacitor (Fig. 5). The advantage of this approach is threefold: (a) the ability to obtain any required capacitance range and (b) to channel most of the current via low ESR capacitors (e.g. film dielectric capacitors) and hence, not be limited by the power dissipation of the voltage-dependent ceramic capacitor, and (c) still maintaining practically infinite capacitance-control resolution.

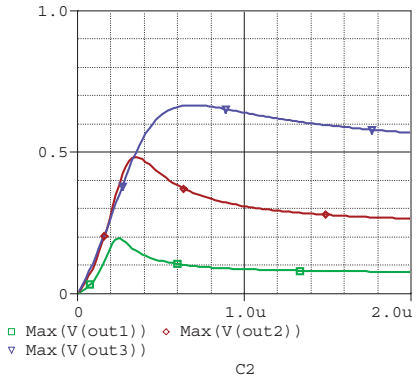

Fig.3. Simulation WPT voltage transfer function as a function of C_s.

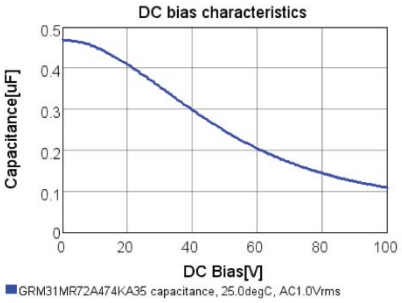

Fig. 4a. Incremental capacitance of GRM31MR72A474KA35 (Murata)

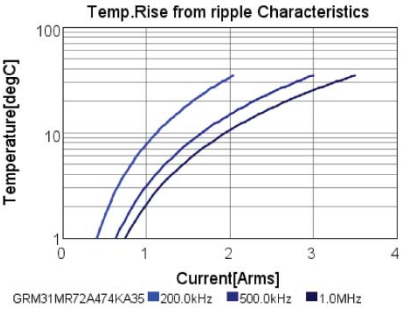

Fig.4b. Temperature rise and a function of current of CC of Fig. 4a.

V. Experimental

The experimental set up (Fig. 6) applied two ceramic capacitors types (Murata, GRM31MR72A474KA35 and TDK, FG28X7R1H474KRT06, connected in parallel) and then in series with a DC blocking capacitor (C3, MKP). The capacitance of voltage-controlled capacitor assembly was adjusted by a variable DC power supply via large resistance RB. The voltage dependence of the capacitance of two of the experimentally applied assemblies are depicted in Fig. 6.

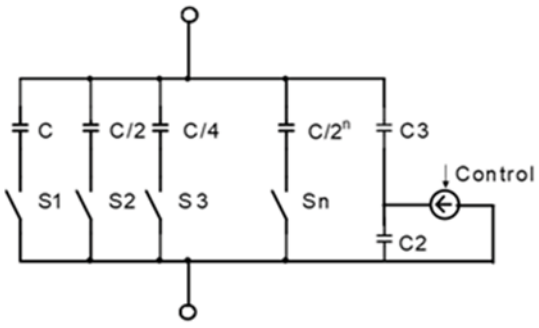

Fig 5. Proposed discrete/continuous controlled-capacitance assembly.

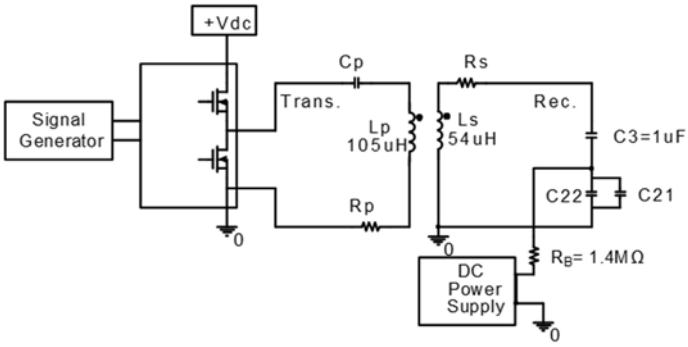

Fig.6. Experimental setup.

The transmitter antenna was driven by a half-bridge driver (TI, UCC27201AEVM-328). The antennas' parameters were: diameters 18cm; transmitter antenna number of turns 33; receiver antenna number of turns: 30. Other parameters are given above. Fig. 8 is a photo of the experimental antennas.

Test results for k=0.438 and 0.646 (Fig. 9) verify the analytical and simulation predictions. The equivalent input rms voltage was calculated by the first harmonic approximation method: $V_{in}= \sqrt{2}\, V_{DC}/\pi$.

With a 20V DC input voltage the output voltage was 6.7V and the efficiency was 86%.

VI. Conclusion

The proposed voltage-dependent capacitor tuning method for WPT systems is made possible by the ability of the series capacitor at the secondary to adjust the power transfer. The analytical consideration, backed by simulation and validated by experiments, show that commercial ceramic capacitors can be utilized to materialize the proposed approach.

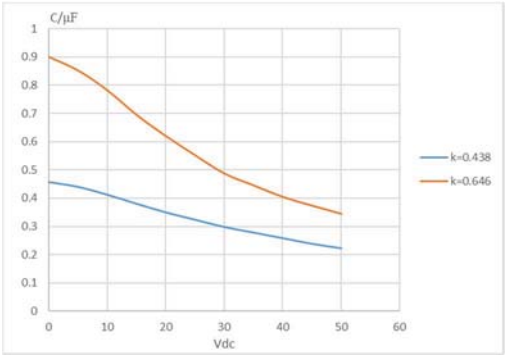

Fig. 7. Capacitance as a function of bias voltage of the ceramic capacitors assembly used in the k= 0.646 (upper curve) and k= 0.438 experiments.

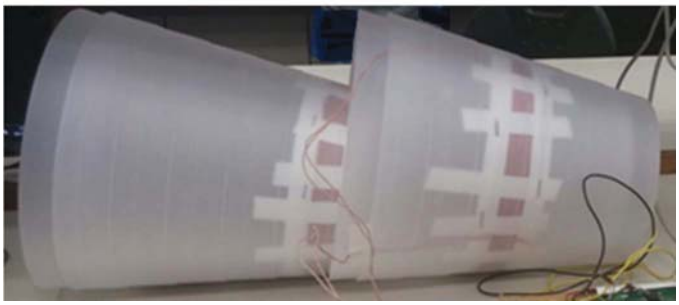

Fig. 8. The experimental antennas.

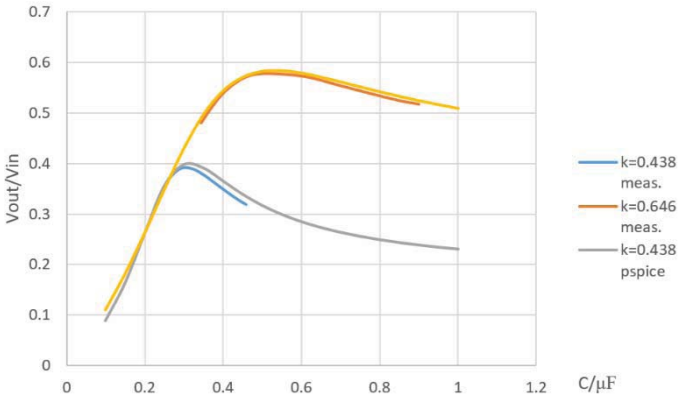

Fig. 9. Simulation and experimental results. Upper curves: k=0.646; Lower curves: k=0.438. Measured data are lower than simulated.

REFERENCES

[1] S. Y. R. Hui, "Past, present and future trends of non-radiative wireless power transfer," in CPSS Transactions on Power Electronics and Applications, vol. 1, no. 1, pp. 83-91, Dec. 2016.

[2] T. Imura, H. Okabe and Y. Hori, "Basic experimental study on helical antennas of wireless power transfer for Electric Vehicles by using magnetic resonant couplings," 2009 IEEE Vehicle Power and Propulsion Conference, Dearborn, MI, 2009, pp. 936-940.

[3] T. Kojiya, F. Sato, H. Matsuki and T. Sato, "Construction of non-contacting power feeding system to underwater vehicle utilizing electromagnetic induction," Europe Oceans 2005, Brest, France, 2005, pp. 709-712 Vol. 1.

[4] T. Kojiya, F. Sato, H. Matsuki and T. Sato, "Construction of non-contacting power feeding system to underwater vehicle utilizing electromagnetic induction," Europe Oceans 2005, Brest, France, 2005, pp. 709-712 Vol. 1.

[5] S. Y. R. Hui, "Past, present and future trends of non-radiative wireless power transfer," in CPSS Transactions on Power Electronics and Applications, vol. 1, no. 1, pp. 83-91, Dec. 2016.

[6] T. Imura, H. Okabe and Y. Hori, "Basic experimental study on helical antennas of wireless power transfer for Electric Vehicles by using magnetic resonant couplings," 2009 IEEE Vehicle Power and Propulsion Conference, Dearborn, MI, 2009, pp. 936-940.

[7] T. Kojiya, F. Sato, H. Matsuki and T. Sato, "Construction of non-contacting power feeding system to underwater vehicle utilizing electromagnetic induction," Europe Oceans 2005, Brest, France, 2005, pp. 709-712 Vol. 1.

[8] S. Y. R. Hui, W. Zhong and C. K. Lee, "A Critical Review of Recent Progress in Mid-Range Wireless Power Transfer," in IEEE Transactions on Power Electronics, vol. 29, no. 9, pp. 4500-4511, Sept. 2014.

[9] H. Aliabadi1 and M. Zarif, “Design and Construct a System of Auto Tuning for Wireless Power Transmission Systems,” Majlesi Journal of Energy Management Vol. 5, No. 3, September 2016, pp. 1-5.

Y. Jiang et al., "An optimal parameters design methodology of series-series resonant tank of wireless power transmission system for battery charging," 2017 IEEE Applied Power Electronics Conference and Exposition (APEC), Tampa, FL, 2017, pp. 1600-1605.

[10] R. L. Steigerwald, "A comparison of half-bridge resonant converter topologies," 1987 2nd IEEE Applied Power Electronics Conference and Exposition, San Diego, CA USA, 1987, pp. 135-144